Exchange and correlation in silicon

Randolph Q. Hood* and M. Y. Chou
School of Physics, Georgia Institute of Technology, Atlanta, Georgia 30332-0430

A. J. Williamson,† G. Rajagopal, and R. J. Needs
Cavendish Laboratory, Madingley Road, Cambridge CB3 0HE, United Kingdom
(Received 7 October 1997)

A combination of the coupling constant integration technique and the quantum Monte Carlo method is used to investigate the most relevant quantities in Kohn-Sham density-functional theory. Variational quantum Monte Carlo is used to construct realistic many-body wave functions for diamond-structure silicon at different values of the Coulomb coupling constant. The exchange-correlation energy density along with the coupling constant dependence and the coupling-constant-integrated form of the pair-correlation function, the exchange-correlation hole, and the exchange-correlation energy are presented. Comparisons of these functions are made with results obtained from the local-density approximation, the average density approximation, the weighted density approximation, and the generalized gradient approximation. We discuss reasons for the success of the local-density approximation. The insights provided by this approach will make it possible to carry out stringent tests of the effectiveness of exchange-correlation functionals and in the long term aid in the search for better functionals. [S0163-1829(98)02115-8]

I. INTRODUCTION

Within the past decade, great strides have been made in predicting theoretically the detailed behavior of electrons in matter, which has brought about a deeper understanding of the nature and properties of real materials. A fundamental obstacle to further advances is the difficulty of treating electron correlation effects in a fully adequate fashion. This is an old problem, having plagued us since the dawn of quantum mechanics, and in the process of addressing this issue various methods have been put forward, among which are many-body perturbation theory, the Hartree-Fock approximation, and density-functional theory. Density-functional theory has proved the most popular of these techniques, both because of its relatively low computational cost for the accuracy of the results obtained, and its wide range of applicability in areas spanning from materials science to biology.

The Kohn-Sham formulation of density-functional theory is the primary method used in electronic structure calculations for treating the many-body effects in solids. In this approach the true many-body system is mapped into a fictitious noninteracting system, whose solution yields the exact ground-state density and energy of the many-body system, provided one knows the functional form of the exchange-correlation energy $E_{\rm xc}[n]$. Since the form of this functional is currently unknown, approximations have been devised, the most ubiquitous being the local-density approximation (LDA), where $E_{\rm xc}$ is written as an integral of a local function of the density with a value at each point in space given by that of a homogeneous electron gas. Despite the seemingly crude nature of this approximation, this approach has been successful in many systems, including those that have rapidly varying densities. However, when qualitative and quantitative discrepancies between experiment and theory in solids arise it is difficult to improve upon the LDA systematically, although several schemes have been devised.[1,2]

Rather than attempting to model the functional form of $E_{\rm xc}[n]$ directly, many schemes for going beyond the LDA start by breaking $E_{\rm xc}$ into constituent contributions using known relations. Physical intuition and experience is then used to model the different terms. For instance, in the average density approximation (ADA) a model is proposed for the exchange-correlation hole, while the weighted density approximation (WDA) models the pair-correlation function.[1] Other procedures break $E_{\rm xc}$ into exchange and correlation contributions,[3,4] while hybrid schemes[5–7] describe how the Coulomb coupling constant dependence of the exchange-correlation energy influences $E_{\rm xc}$. Unfortunately there are very few calculations of the form of these functions in real solids.[8] A careful numerical study of these functions can reveal individual trends and behaviors that may suggest a practical approach for going beyond the LDA and provide a testing ground for the intricacies of existing and future models.

We have used coupling constant integration and variational quantum Monte Carlo (VMC) techniques to calculate the quantities of central importance in density-functional theory that contribute to the exchange-correlation energy for a realistic inhomogeneous solid, namely, diamond structure silicon. This procedure utilizes the exact relationship[9] between the exchange-correlation energy, $E_{\rm xc}$, and the ground-state many-electron wave functions Ψ_λ associated with different values of the Coulomb-coupling constant, λ. This relationship is here written in terms of four equations. The coupling-constant-integrated pair-correlation function $\overline{g}(\mathbf{r},\mathbf{r}')$, the exchange-correlation hole $\rho_{\rm xc}(\mathbf{r},\mathbf{r}')$, and the exchange-correlation energy density $e_{\rm xc}(\mathbf{r})$ are related by[10]

$$e_{\rm xc}(\mathbf{r}) = \frac{n(\mathbf{r})}{2}\int d\mathbf{r}'\frac{\rho_{\rm xc}(\mathbf{r},\mathbf{r}')}{|\mathbf{r}-\mathbf{r}'|}, \tag{1}$$

$$\rho_{\rm xc}(\mathbf{r},\mathbf{r}')=n(\mathbf{r}')\{\bar{g}(\mathbf{r},\mathbf{r}')-1\}. \quad (2)$$

The total exchange-correlation energy $E_{\rm xc}$ is obtained by integrating $e_{\rm xc}(\mathbf{r})$ over all space. Writing $\bar{g}$ in terms of its constituent spin components

$$\bar{g}(\mathbf{r},\mathbf{r}')=\sum_{\alpha,\beta}\frac{n_\alpha(\mathbf{r})n_\beta(\mathbf{r}')}{n(\mathbf{r})n(\mathbf{r}')}\bar{g}_{\alpha\beta}(\mathbf{r},\mathbf{r}') \quad (3)$$

yields an equation involving the many-electron wave functions:

$$\bar{g}_{\alpha\beta}(\mathbf{r},\mathbf{r}')=\frac{N(N-1)}{n_\alpha(\mathbf{r})n_\beta(\mathbf{r}')}\int_0^1 d\lambda\int d\mathbf{x}_3\cdots d\mathbf{x}_N|\Psi_\lambda \times(\mathbf{r}\alpha,\mathbf{r}'\beta,\mathbf{x}_3,\ldots,\mathbf{x}_N)|^2, \quad (4)$$

where N is the number of electrons, $n_\alpha(\mathbf{r})$ is the electronic density for spin α, and $\mathbf{x}_i$ denotes the ith electron's spatial and spin components. In an unpolarized system such as silicon Eq. (3) reduces to $\bar{g}=\frac{1}{4}\Sigma_{\alpha,\beta}\bar{g}_{\alpha\beta}$. The electronic density of each Ψ_λ must equal the density at full coupling ($\lambda=1$). This condition can be ensured by adding an additional external potential $v_\lambda(\mathbf{r})$ to the many-body Hamiltonian in which the electron-electron interaction is multiplied by λ.

In a recent paper[8] we briefly described our method. Here we present new results along with a more complete description of our procedure. In Sec. II we provide the details of our approach for calculating the different quantities. We describe our λ-dependent Hamiltonian and wave functions, and an efficient method for Monte Carlo sampling of the λ-dependent pair-correlation function, from which all the other functions can be calculated. In Sec. III we discuss the form of the pair-correlation function, presenting both its exchange and correlation contributions. We describe the exchange-correlation hole and how its λ dependence influences its shape. The Monte Carlo calculated $e_{\rm xc}(\mathbf{r})$ is compared with the form obtained in the LDA, WDA, and ADA, and reasons for the success of the LDA are discussed. The λ dependence of the exchange-correlation energy is presented in several approximations and compared with our Monte Carlo results. Details for obtaining $e_{\rm xc}(\mathbf{r})$ from the Monte Carlo sampled pair-correlation function are presented in the Appendix.

II. CALCULATIONAL METHODS

A. Hamiltonian

For our calculations we used a simulation cell consisting of $3\times3\times3$ primitive fcc unit cells of the diamond lattice, and containing 216 valence electrons. At a value of the Coulomb coupling constant λ the Hamiltonian used in our simulations has the form

$$\hat{H}_\lambda=-\sum_i\frac{1}{2}\nabla_i^2+\sum_i\hat{V}_{{\rm ext}\,i}+\lambda\hat{H}_{e\text{-}e}+\sum_i v_\lambda(\mathbf{r}_i), \quad (5)$$

where a norm-conserving nonlocal LDA pseudopotential $\hat{V}_{\rm ext}$ was used to model the core electrons. We used an electron-electron interaction of the form

$$\hat{H}_{e\text{-}e}=\sum_{i>j}f(\mathbf{r}_i-\mathbf{r}_j)+\sum_i\int d\mathbf{r}n(\mathbf{r})\left[\frac{1}{|\mathbf{r}_i-\mathbf{r}|}-f(\mathbf{r}_i-\mathbf{r})\right], \quad (6)$$

where $f(\mathbf{r})=1/r$ if $\mathbf{r}$ is inside the Wigner-Seitz cell of the simulation cell, and is zero otherwise. The condition that f vanishes outside that Wigner-Seitz cell of the simulation cell centered on the particle in question is equivalent to the ''nearest image'' convention which is widely used in computer simulations. This interaction gives smaller Coulomb finite-size effects than the standard Ewald interaction when finite simulation cells and periodic boundary conditions are used to simulate effectively infinite systems.[11] The total electron-electron energy is the expectation value of $\hat{H}_{e\text{-}e}$ minus a double counting term for the electrostatic interactions. The exchange-correlation energy density $e_{\rm xc}(\mathbf{r})$ has smaller finite-size effects when $f(\mathbf{r}-\mathbf{r}')$ is used for $1/|\mathbf{r}-\mathbf{r}'|$ in Eq. (1) instead of the periodic Ewald interaction.[11] Finite-size effects can alter the λ-dependence of quantities such as $U_{\rm xc}^\lambda$, where $E_{\rm xc}=\int_0^1 U_{\rm xc}^\lambda d\lambda$. When we performed calculations with the Ewald form of the electron-electron interaction, we found with increasing system size a change in the shape of the curve $U_{\rm xc}^\lambda$ versus λ in addition to a constant λ-independent shift. Using the electron-electron interaction of Eq. (6) reduced the magnitude of these finite-size effects.

The ground-state charge density $n(\mathbf{r})$ that appears in $\hat{H}_{e\text{-}e}$ can be obtained self-consistently by repeating the calculation. However, we found that the solution was insensitive to the precise form of the density. In the case of silicon the LDA density agrees closely with experiment[12] and is indistinguishable (within statistical noise) from the density we obtained at $\lambda=1$ in VMC using either the Ewald interaction for $\hat{H}_{e\text{-}e}$ or the form in Eq. (6) with the LDA density. At all values of λ the latter form of $\hat{H}_{e\text{-}e}$ was used.

As an initial approximation for v_λ we used

$$v_\lambda(\mathbf{r})=(1-\lambda)\int d\mathbf{r}'\frac{n(\mathbf{r}')}{|\mathbf{r}-\mathbf{r}'|}+v_{{\rm xc},\lambda=1}^{\rm LDA}(n(\mathbf{r}))-v_{{\rm xc},\lambda}^{\rm LDA}(n(\mathbf{r})),$$

which would ensure that the density was independent of λ in an LDA calculation. The value of $v_{{\rm xc},\lambda}^{\rm LDA}(n)$ was obtained from the exact scaling relation,[13] $v_{{\rm xc},\lambda}^{\rm LDA}(n)=\lambda^2 v_{{\rm xc},\lambda=1}^{\rm LDA}(n/\lambda^3)$. This form of v_λ yielded charge densities in close agreement with $n_{\lambda=1}(\mathbf{r})$. This approximation should be reliable for systems where the LDA provides an accurate prediction of the ground-state density, which is the case in silicon.[12] The small residual deviations from the LDA density[14] were reduced by iteratively modifying the v_λ potentials and lastly by making a very small adjustment to the one-body functions in the Jastrow term of the wave functions, which caused no discernible change in the total energy. The root-mean-square deviation of the final n_λ from the LDA density was less than 0.58% for all values of λ.

B. Wave function

At each value of λ the wave function used in the VMC calculations was of the Slater-Jastrow form:

$$\Psi_\lambda = D^\uparrow D^\downarrow \exp\left[-\sum_{i>j} u^\lambda(|\mathbf{r}_i - \mathbf{r}_j|) + \sum_i \chi^\lambda(\mathbf{r}_i) \right], \quad (7)$$

where $D^\uparrow$ and $D^\downarrow$ are Slater determinants containing single-particle orbitals obtained from an LDA calculation. The two-body term in the Jastrow factor is written[15] in two parts:

$$u^\lambda(r) = u_0^\lambda(r) + f^\lambda(r),$$

where $u_0^\lambda(r)$ is fixed and $f^\lambda(r)$ contains variational parameters. The fixed part of u has the form

$$u_0^\lambda(r) = \frac{A}{r}\left[1 - \exp\left(-\frac{r}{F^\lambda} \right) \right] \exp\left(-\frac{r^2}{L_0^2} \right)$$

and the λ dependent cusp conditions are satisfied by setting $F^\lambda = \sqrt{A/\lambda}$ for antiparallel spins and $F^\lambda = \sqrt{2A/\lambda}$ for parallel spins. The value of L_0 was set equal to $0.25 L_{\mathrm{WS}}$ where L_{WS} is the radius of the largest sphere entirely contained within the Wigner-Seitz cell of the simulation cell. This choice of L_o insured that $u_0^\lambda(L_{\mathrm{WS}})$ was effectively zero. A separate VMC calculation with $f^\lambda(r)$ set to zero was used to determine the optimal value of A. The variable part of u^λ has the form

$$f^\lambda(r) = B^\lambda\left(\frac{L_{\mathrm{WS}}}{2} + r \right)(L_{\mathrm{WS}} - r)^2 + r^2(L_{\mathrm{WS}} - r)^2 \sum_{l=0}^{M} \alpha_l^\lambda T_l(\bar{r}), \quad 0 \le r \le L_{\mathrm{WS}},$$

$$= 0, \quad r > L_{\mathrm{WS}},$$

where B^λ and the α_l^λ are variational coefficients that depend on the relative spins of the electrons, T_l is the lth Chebyshev polynomial, and

$$\bar{r} = \frac{2r - L_{\mathrm{WS}}}{L_{\mathrm{WS}}}.$$

The χ^λ function, expanded in a Fourier series, was chosen to have the full symmetry of the diamond structure:

$$\chi^\lambda(\mathbf{r}) = \sum_s c_s^\lambda \left(\sum_{\mathbf{G} \in s} P_{\mathbf{G}} e^{i\mathbf{G}\cdot\mathbf{r}} \right),$$

where s labels a star of reciprocal lattice $\mathbf{G}$-vectors of the primitive cell and $P_{\mathbf{G}}$ is a phase factor associated with the nonsymmorphic symmetry operations. At each value of λ in our VMC calculations we used a total of six nonzero coefficients c_s^λ in χ^λ and eight parameters for both the parallel- and antiparallel-spin u^λ functions giving a total of 22 parameters in the wave functions, which were optimized by minimizing the variance of the energy[16] following the methodology described in Ref. 17. Comparison with diffusion Monte Carlo results showed that our optimized wave function for $\lambda = 1$ retrieves 85% of the fixed-node correlation energy.

C. Calculation of pair-correlation function

To obtain the quantities in Eqs. (1)–(4) requires an accurate representation of $g_{\alpha\beta}^\lambda$ throughout *all* of the the six-dimensional space $\mathbf{r} \times \mathbf{r}'$, in contrast to previous calculations which obtained $g_{\alpha\beta}^{\lambda=1}$ at only a few points.[18] We have found that an efficient way to calculate and store this information is to expand $g_{\alpha\beta}^\lambda$ as a product of single-particle functions. The number of independent coefficients in this expansion was considerably reduced by making use of the full space group symmetry of the crystal.

From Eq. (4) the symmetries satisfied by $g_{\alpha\beta}^\lambda$ follow from the symmetries of Ψ_λ. At each λ the many-body Hamiltonian H_λ in Eq. (5) and $|\Psi_\lambda|^2$, the modulus of our Slater-Jastrow wave function of Eq. (7), are invariant under the following: $\mathcal{S}_1$, a translation of any single electron by an arbitrary Bravais lattice vector $\mathbf{T}$ of the simulation cell; $\mathcal{S}_2$, simultaneous operation on all the electron coordinates by an arbitrary element $\{R|\boldsymbol{\tau}_R + \mathbf{t}\}$ of the crystallographic space group O_h^7 of the diamond structure; $\mathcal{S}_3$, an arbitrary permutation of electron coordinates with the same spin, and $\mathcal{S}_4$, time-reversal symmetry, i.e., complex conjugation.

Symmetry $\mathcal{S}_1$ results from the periodic boundary conditions imposed on the simulation cell consisting of $3 \times 3 \times 3$ primitive fcc unit cells of the diamond lattice, from which it follows that

$$g_{\alpha\beta}^\lambda(\mathbf{r},\mathbf{r}') = g_{\alpha\beta}^\lambda(\mathbf{r}+\mathbf{T},\mathbf{r}') = g_{\alpha\beta}^\lambda(\mathbf{r},\mathbf{r}'+\mathbf{T}) \quad (8)$$

with

$$\mathbf{T} = l_1 3\mathbf{a}_1 + l_2 3\mathbf{a}_2 + l_3 3\mathbf{a}_3,$$

where the $\mathbf{a}_i$ are a set of primitive vectors for the direct fcc lattice and l_1, l_2, l_3 are integers. Since the operator associated with a coordinate transformation $\{R|\boldsymbol{\tau}_R + \mathbf{t}\}$ acting on each electron coordinate is unitary it follows from $\mathcal{S}_2$ that

$$g_{\alpha\beta}^\lambda(\mathbf{r},\mathbf{r}') = g_{\alpha\beta}^\lambda(R\mathbf{r} + \boldsymbol{\tau}_R + \mathbf{t}, R\mathbf{r}' + \boldsymbol{\tau}_R + \mathbf{t}). \quad (9)$$

From Eq. (4) it follows that $g_{\alpha\beta}^\lambda(\mathbf{r},\mathbf{r}')$ is real, while $\mathcal{S}_3$ along with the form of the VMC wave function in Eq. (7) dictate that it satisfy the symmetry relation

$$g_{\alpha\beta}^\lambda(\mathbf{r},\mathbf{r}') = g_{\beta\alpha}^\lambda(\mathbf{r}',\mathbf{r}).$$

Since $g_{\alpha\beta}^\lambda(\mathbf{r},\mathbf{r}')$ is a continuous function of the spatial coordinates, it can be expanded in a product of a complete set of single particle orthonormal functions. Equation (9) shows it is advantageous in this expansion to use basis functions of the unitary irreducible representations of the group O_h^7. These are denoted[19] $\phi_{tr,m}^{\mathbf{k}p}(\mathbf{r})$, where $\mathbf{k}$ is a $\mathbf{k}$ vector of the fcc Brillouin zone consistent with the periodic boundary conditions, p is an index for the representations of the group $\mathcal{G}(\mathbf{k})$ of the wave vector $\mathbf{k}$, $t \in \{1,2,\ldots,M(\mathbf{k})\}$ is an index over $M(\mathbf{k})$ inequivalent $\mathbf{k}$ vectors that lie in the ''star'' of $\mathbf{k}$, $r \in \{1,2,\ldots,d_p\}$ is the row index of the d_p dimensional ''relevant'' p representation of $\mathcal{G}(\mathbf{k})$, and m is an index for basis functions that transform according to the same representation but are linearly independent. A matrix element in the expansion takes the form

$$\int d\mathbf{r} \int d\mathbf{r}' \, \phi_{tr,m}^{\mathbf{k}p*}(\mathbf{r}) g_{\alpha\beta}^\lambda(\mathbf{r},\mathbf{r}') \phi_{t'r',m'}^{\mathbf{k}'p'}(\mathbf{r}'). \quad (10)$$

From $\mathcal{S}_1$ and Bloch's theorem, which is satisfied by the basis functions ϕ, this matrix element will be nonzero only if $\mathbf{k}$ and $\mathbf{k}'$ are reciprocal lattice vectors of the simulation cell, which Eq. (8) implies they satisfy:

$$\mathbf{k}=m_1\tfrac{1}{3}\mathbf{b}_1+m_2\tfrac{1}{3}\mathbf{b}_2+m_3\tfrac{1}{3}\mathbf{b}_3,$$

where $\mathbf{b}_i$ are primitive vectors for the reciprocal lattice and $m_i\in\{-1,0,1\}$. These 27 $\mathbf{k}$ vectors can be grouped into four distinct stars. By periodicity both integrals in Eq. (10) can be performed over a simulation cell volume. Symmetry $\mathcal{S}_2$ along with the ''orthogonality theorem for matrix representations''[20] imply that

$$\int d\mathbf{r}\int d\mathbf{r}'\,\phi^{\mathbf{k}p*}_{tr,m}(\mathbf{r})g^{\lambda}_{\alpha\beta}(\mathbf{r},\mathbf{r}')\phi^{\mathbf{k}'p'}_{t'r',m'}(\mathbf{r}')$$
$$=g^{\lambda,\mathbf{k}p}_{\alpha\beta;m,m'}\delta_{\mathbf{k},\mathbf{k}'}\delta_{p,p'}\delta_{t,t'}\delta_{r,r'}.$$

The expansion therefore takes the form

$$g^{\lambda}_{\alpha\beta}(\mathbf{r},\mathbf{r}')=\sum_{\mathbf{k}p}\sum_{m,m'}g^{\lambda,\mathbf{k}p}_{\alpha\beta;m,m'}\sum_{t=1}^{M(\mathbf{k})}\sum_{\mathbf{r}=1}^{d_p}\phi^{\mathbf{k}p}_{tr,m}(\mathbf{r})\phi^{\mathbf{k}p*}_{tr,m'}(\mathbf{r}'),\tag{11}$$

where the leftmost sum is over the four inequivalent $\mathbf{k}$ vectors, each of which has a corresponding nontrivial point group $\mathcal{G}_0(\mathbf{k})$, and the coefficients are independent of the row tr of the representation. From $\mathcal{S}_4$ and the inversion symmetry of the group O_h^7 the phase factor of the orbitals ϕ can be chosen such that $\phi^{\mathbf{k}p*}_{tr,m}(\mathbf{r})=\phi^{\mathbf{k}p}_{t'r,m}(\mathbf{r})$, where $R_t\mathbf{k}=-R_{t'}\mathbf{k}$, from which it follows that $\Sigma_{t=1}^{M(\mathbf{k})}\Sigma_{\mathbf{r}=1}^{d_p}\phi^{\mathbf{k}p}_{tr,m}(\mathbf{r})\phi^{\mathbf{k}p*}_{tr,m'}(\mathbf{r}')$ is a real function of $(\mathbf{r},\mathbf{r}')$. Thus $g^{\lambda,\mathbf{k}p}_{\alpha\beta;m,m'}$ is a real symmetric function of m,m'. In an unpolarized system like silicon the coefficients $g^{\lambda,\mathbf{k}p}_{\alpha\beta;m,m'}$ in the expansion of $g^{\lambda}_{\alpha\beta}(\mathbf{r},\mathbf{r}')$ satisfy $g^{\lambda,\mathbf{k}p}_{\uparrow\uparrow;m,m'}=g^{\lambda,\mathbf{k}p}_{\downarrow\downarrow;m,m'}$ and $g^{\lambda,\mathbf{k}p}_{\uparrow\downarrow;m,m'}=g^{\lambda,\mathbf{k}p}_{\downarrow\uparrow;m,m'}$.

In Eq. (4) one has the freedom to choose which pair of electron coordinates are held fixed when calculating the pair-correlation function. By averaging over each choice the noise in the statistical evaluation of the integral can be considerably reduced. Defining the quantity

$$h^{\lambda,\mathbf{k}p}_{m,m'}(i,j)=2\int d\mathbf{r}_1\cdots d\mathbf{r}_N\frac{\phi^{\mathbf{k}p*}_{11,m}(\mathbf{r}_i)}{n(\mathbf{r}_i)}\frac{\phi^{\mathbf{k}p}_{11,m'}(\mathbf{r}_j)}{n(\mathbf{r}_j)}$$
$$\times|D_{\uparrow}(\mathbf{r}_1,\ldots,\mathbf{r}_{N/2})D_{\downarrow}(\mathbf{r}_{(N/2)+1},\ldots,\mathbf{r}_N)$$
$$\times J_{\lambda}(\mathbf{r}_1,\ldots,\mathbf{r}_N)|^2$$

with the choice $t=1$ and $r=1$, where $i,j\in 1,\ldots,N$, and using the fact that $n_{\alpha}(\mathbf{r})=\frac{1}{2}n(\mathbf{r})$ for all α and $\mathbf{r}$ in silicon, one can derive the equation

$$g^{\lambda,\mathbf{k}p}_{\alpha\beta;m,m'}=\begin{cases}\underbrace{\sum_{i=1}^{\frac{N}{2}}\sum_{j=1}^{\frac{N}{2}}}_{i\neq j}h^{\lambda,\mathbf{k}p}_{m,m'}(i,j)+\underbrace{\sum_{i=\frac{N}{2}+1}^{N}\sum_{j=\frac{N}{2}+1}^{N}}_{i\neq j}h^{\lambda,\mathbf{k}p}_{m,m'}(i,j) & \text{if } \alpha=\beta\\ \sum_{i=1}^{\frac{N}{2}}\sum_{j=\frac{N}{2}+1}^{N}h^{\lambda,\mathbf{k}p}_{m,m'}(i,j)+\sum_{i=\frac{N}{2}+1}^{N}\sum_{j=1}^{\frac{N}{2}}h^{\lambda,\mathbf{k}p}_{m,m'}(i,j) & \text{if } \alpha\neq\beta\end{cases}$$

by inserting our Slater-Jastrow wave function in Eq. (4) where J_{λ} is the exponential Jastrow term appearing in Eq. (7), relabeling dummy indices in the integral, and utilizing $\mathcal{S}_3$. The quantities $h^{\lambda,\mathbf{k}p}_{m,m'}(i,j)$, for all $i,j\in 1,\ldots,N$ with $i\neq j$, are accumulated simultaneously by summing over $\mathcal{N}$ independent configurations distributed according to the square of our Slater-Jastrow wave function using Metropolis sampling:

$$h^{\lambda,\mathbf{k}p}_{m,m'}(i,j)=\frac{2}{\mathcal{N}}\sum_{l=1}^{\mathcal{N}}\frac{\phi^{\mathbf{k}p*}_{11,m}(\mathbf{r}_i^l)}{n(\mathbf{r}_i^l)}\frac{\phi^{\mathbf{k}p}_{11,m'}(\mathbf{r}_j^l)}{n(\mathbf{r}_j^l)}+O\left(\frac{1}{\sqrt{\mathcal{N}}}\right).\tag{12}$$

For a given size of $\mathcal{N}$, the statistical noise in the coefficients $g^{\lambda,\mathbf{k}p}_{\alpha\beta;m,m'}$ was found to be largely independent of the indices. Averaging $g^{\lambda,\mathbf{k}p}_{\alpha\beta;m,m'}$ over different rows tr did not yield a reduction in the ratio of statistical noise to computational time of $g^{\lambda}_{\alpha\beta}(\mathbf{r},\mathbf{r}')$, instead it was more efficient to reduce the noise by increasing $\mathcal{N}$.

We tested the rate of convergence of the expansion of $g^{\lambda}_{\alpha\beta}(\mathbf{r},\mathbf{r}')$ in Eq. (11) using basis functions of symmetrized plane waves and LDA orbitals. The symmetrized plane waves were constructed using the projection operator technique[21] with a plane wave cutoff up to 38 Ry. A 23 Ry cutoff was found to be sufficient, corresponding to 82 616 independent coefficients $g^{\lambda,\mathbf{k}p}_{\alpha\beta;m,m'}$ at each value of λ. The LDA orbitals consisted of those occupied and unoccupied orbitals of the ground state of silicon with eigenvalues below an energy cutoff, chosen such that the number of LDA orbitals corresponded to the number of symmetrized plane waves. These LDA orbitals displayed a much slower rate of convergence. Symmetrized plane waves had the computational advantage over LDA orbitals of requiring no more than 48 plane waves per basis function. This resulted in less computer storage and a faster computation of the terms in Eq. (12). At each λ all of the coefficients were accumulated simultaneously with the Monte Carlo metropolis method using approximately 5.8 million statistically independent configurations. For $\lambda=0$, $g^{\lambda,\mathbf{k}p}_{\alpha\beta;m,m'}$ can be generated directly from the single-particle orbitals of the determinant in Eq. (7). By comparing the Monte Carlo sampled and directly calculated functions we estimated the statistical error in $\bar{g}$ to be

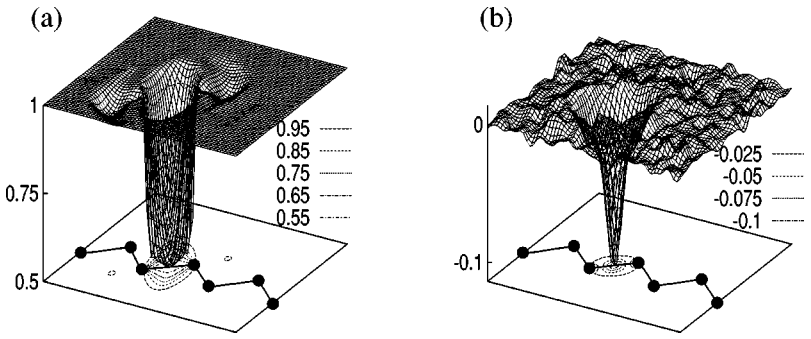

FIG. 1. Plots in VMC of (a) g_x, and (b) $\overline{g_c}$ in the (110) plane passing through the atoms with one electron fixed at the bond center. The atoms and bonds in the (110) plane are schematically represented.

between 1% and 6%. The noise was largest where the electronic density takes its smallest value, and smallest where the electronic density was largest. These estimates were consistent with the deviations observed at $\lambda=1$ in $g^{\lambda,\mathbf{k}p}_{\alpha\beta;m,m'}$ calculated with two different sets of 5.8 million statistically independent configurations. We also used direct calculations to investigate the effects of the finite size of the simulation cell on $g^{\lambda=0,\mathbf{k}p}_{\alpha\beta;m,m'}$, which were found to be unimportant.

The integral over λ in Eq. (4) was evaluated numerically using five values of λ: 0, $\frac{1}{4}$, $\frac{1}{2}$, $\frac{3}{4}$, and 1. Since the basis functions $\phi^{\mathbf{k}p}_{tr,m}(\mathbf{r})$ that appear in Eq. (11) are independent of λ, the integral involved merely a weighted average over λ of the coefficients $g^{\lambda,\mathbf{k}p}_{\alpha\beta;m,m'}$. The accuracy of the value of the integral obtained with five values of λ was investigated by studying the λ dependence of various quantities. With increasing λ the exchange-correlation energy $U^{\lambda}_{\mathrm{xc}}$, where $E_{\mathrm{xc}}=\int_0^1 U^{\lambda}_{\mathrm{xc}}d\lambda$, was found to decrease smoothly and monotonically as has been predicted by Levy and Perdew.[22] This can be seen in Fig. 7, which will be discussed later. Other quantities investigated: the Jastrow term in the many-body wave function and $g^{\lambda}_{\alpha\beta}$, displayed a smooth monotonic dependence on λ. As a further test, the identity

$$T^{\lambda=0}+E_{\mathrm{xc}}=T^{\lambda=1}+U^{\lambda=1}_{\mathrm{xc}} \tag{13}$$

was found to hold within 0.1%, where $T^{\lambda=1}$ is the fully interacting kinetic energy and $T^{\lambda=0}$ is the noninteracting kinetic energy appearing in density-functional theory. Fewer than five values of λ was insufficient to satisfy this equation.

D. Calculation of the exchange-correlation energy density

The exchange-correlation energy density $e_{\mathrm{xc}}(\mathbf{r})$ was calculated using two techniques. One approach involved direct Monte Carlo metropolis sampling with the Slater-Jastrow wave function for each of the five values of λ using the equation

$$e_{\mathrm{xc}}(\mathbf{r})=\frac{1}{2}\int_0^1 d\lambda\sum_i^N\sum_{j\neq i}^N\int d\mathbf{x}_1\cdots d\mathbf{x}_N\,\delta(\mathbf{r}-\mathbf{r}_i)\times f(\mathbf{r}-\mathbf{r}_j)|\Psi_\lambda(\mathbf{x}_1,\mathbf{x}_2,\ldots,\mathbf{x}_N)|^2-\frac{1}{2}\int d\mathbf{r}'\,n(\mathbf{r})n(\mathbf{r}')f(\mathbf{r}-\mathbf{r}'),$$

which follows from combining Eqs. (1)–(4) and replacing the Ewald interaction, $1/|\mathbf{r}-\mathbf{r}'|$, with $f(\mathbf{r}-\mathbf{r}')$ to reduce finite-size effects. The other approach involved a numerical integration over λ of the expansion in Eq. (11) for $g^{\lambda}_{\alpha\beta}(\mathbf{r},\mathbf{r}')$, followed by an analytic integration over the variable $\mathbf{r}'$, that appears in Eq. (1). Both approaches yield identical results in the limit of an infinite cutoff in the symmetrized plane waves of the expansion of Eq. (11), and an infinite number of statistically independent configurations used in the Monte Carlo metropolis sampling. For a finite cutoff the expansion in Eq. (11) results in an incorrect cusp[23] in $g^{\lambda}_{\alpha\beta}(\mathbf{r},\mathbf{r}')$ when $\alpha\neq\beta$ and $\mathbf{r}\rightarrow\mathbf{r}'$. Sampling $g^{\lambda}_{\alpha\beta}(\mathbf{r},\mathbf{r}')$ with a finite number of configurations results in a statistical violation of the sum rule:

$$4\pi\int dRR^2\rho^{\lambda}_{\mathrm{xc},\alpha\beta}(\mathbf{r},R)=-\delta_{\alpha,\beta} \tag{14}$$

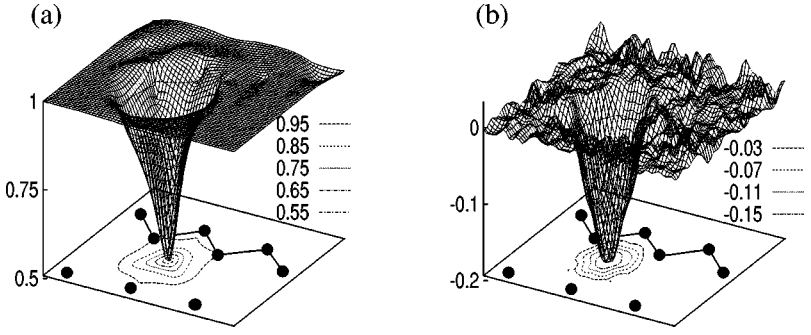

FIG. 2. Plots in VMC of (a) g_x, and (b) $\overline{g_c}$ in the (110) plane passing through the atoms with one electron fixed at the tetrahedral interstitial site. The atoms and bonds in the (110) plane are schematically represented.

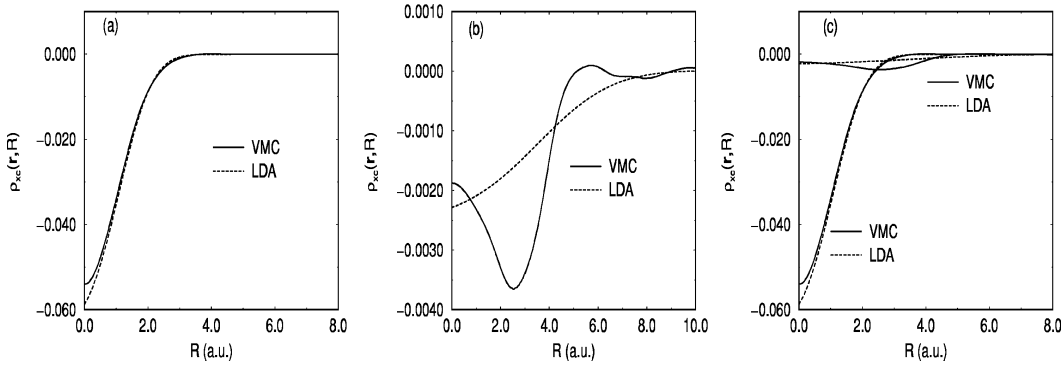

FIG. 3. The spherically averaged exchange-correlation hole in VMC and LDA with (a) one electron fixed at the bond center, (b) one electron fixed at the tetrahedral interstitial site, and (c) plots (a) and (b) superimposed.

for the spherically averaged exchange-correlation hole at λ where

$$\rho^{\lambda}_{\mathrm{xc},\alpha\beta}(\mathbf{r},R)=\frac{1}{4\pi}\int_{\Omega}d\mathbf{r}'\,n(\mathbf{r}')\{g^{\lambda}_{\alpha\beta}(\mathbf{r},\mathbf{r}')-1\},$$

$$\Omega:|\mathbf{r}-\mathbf{r}'|=R.$$

This violation is a result of the R^2 term in the integral of Eq. (14), which magnifies the small statistical errors in $g^{\lambda}_{\alpha\beta}$ at large R that do not cancel completely in the spherical averaging of the exchange-correlation hole. These small fluctuations at large R are also magnified in the evaluation of $e_{\mathrm{xc}}(\mathbf{r})$,

$$e_{\mathrm{xc}}(\mathbf{r})=2\pi n(\mathbf{r})\int_0^1 d\lambda\int dRR\rho^{\lambda}_{\mathrm{xc}}(\mathbf{r},R), \qquad (15)$$

by the presence of R in the integral. Our method for removing these errors is described in the Appendix. With this correction both procedures yield the same statistical error in $e_{\mathrm{xc}}(\mathbf{r})$ when sampled with the same number of statistically independent configurations. This serves as a test of the adequacy of the cutoff in the expansion, Eq. (11), for $g^{\lambda}_{\alpha\beta}(\mathbf{r},\mathbf{r}')$. It reveals that the violation of the cusp condition in $g^{\lambda}_{\alpha\beta}(\mathbf{r},\mathbf{r}')$ when $\alpha\neq\beta$ as $\mathbf{r}\rightarrow\mathbf{r}'$ has a smaller effect on the errors in $e_{\mathrm{xc}}(\mathbf{r})$ than our statistical noise, partially because of the R factor in Eq. (15) that goes to zero where the cusp condition is violated. There was a root-mean square deviation of 0.5% between both evaluations of $e_{\mathrm{xc}}(\mathbf{r})$. This is consistent with an estimate of the statistical noise obtained by comparing the two VMC evaluations of $e^{\lambda=0}_{\mathrm{xc}}(\mathbf{r})$ with the exact quantity.

III. RESULTS AND ANALYSIS

Recent studies[8,18] of the pair-correlation function in bulk silicon have discussed the form of $g^{\lambda=1}_{\alpha\beta}(\mathbf{r},\mathbf{r}')$ and $\overline{g}_{\alpha\beta}(\mathbf{r},\mathbf{r}')$. Here we consider that the pair-correlation function can be broken up into exchange g_{x} and correlation $\overline{g_{\mathrm{c}}}$ contributions $\overline{g}=g_{\mathrm{x}}+\overline{g_{\mathrm{c}}}$ according to the density-functional theory definition,[24] where $g_{\mathrm{x}}=g^{\lambda=0}$ and $\overline{g_{\mathrm{c}}}=\overline{g}-g_{\mathrm{x}}$. Plots of g_{x} and $\overline{g_{\mathrm{c}}}$ around a bond center are shown in Fig. 1, and around the tetrahedral interstitial site in Fig. 2. Analysis of these and other points in silicon reveal that g_{x} tends to be more anisotropic in comparison to $\overline{g_{\mathrm{c}}}$. Comparing Figs. 1 and 2 we see that $\overline{g_{\mathrm{c}}}$ is larger and deeper at the interstitial site than at the bond center. The valence electronic density is over thirty times smaller at the interstitial site than at the bond center. In our study we found that $\overline{g_{\mathrm{c}}}$ tends to be larger and deeper where the electronic density is smaller; the same trend that is observed in a homogeneous electron gas.[25]

From the pair-correlation function the exchange-correlation hole can be easily obtained. In Figs. 3(a) and 3(b) are plots of the spherically averaged exchange-correlation hole around a bond center and an interstitial site respectively. Only the spherical average contributes to the exchange-correlation energy. The percentage deviation from the LDA is smaller at the bond center than at the interstitial site, where the LDA gives a poor approximation. The size of the deviation from the LDA has the same order of magnitude around both points as can be seen in Fig. 3(c) where the exchange-correlation holes are superimposed on a plot with the same scale and reflected by the fact that the value of the exchange-correlation energy density per particle,

$$\epsilon_{\mathrm{xc}}(\mathbf{r})=2\pi\int dRR\rho_{\mathrm{xc}}(\mathbf{r},R),$$

has the same magnitude, as shown in Table I. The absolute

TABLE I. Monte Carlo (VMC) and local-density approximation (LDA) values for the exchange-correlation energy density per particle $\epsilon_{\mathrm{xc}}(\mathbf{r})$ and $e_{\mathrm{xc}}(\mathbf{r})=n(\mathbf{r})\epsilon_{\mathrm{xc}}(\mathbf{r})$ at the bond center and the tetrahedral interstitial sites in silicon. The energies are in atomic units.

Position	$\epsilon_{\mathrm{xc}}(\mathbf{r})$		$e_{\mathrm{xc}}(\mathbf{r})$		
$\mathbf{r}$	VMC	LDA	VMC	LDA	% error in LDA
Bond center	−0.371	−0.381	−0.032 4	−0.033 3	−2.8
Interstitial	−0.166	−0.133	−0.000 459	−0.000 368	19.8

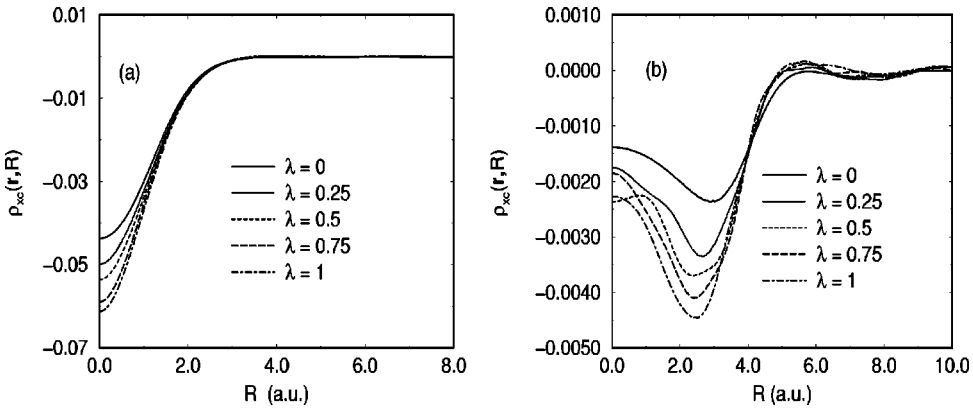

FIG. 4. The spherically averaged exchange-correlation hole in VMC as a function of the Coulomb coupling constant λ ranging from no coupling ($\lambda=0$) to full coupling ($\lambda=1$) with (a) one electron fixed at the bond center, and (b) one electron fixed at the tetrahedral interstitial site.

deviation of $e_{\rm xc}(\mathbf{r})=n(\mathbf{r})\epsilon_{\rm xc}(\mathbf{r})$ in the VMC from the LDA is an order of magnitude larger at the bond center because $n(\mathbf{r})$ is over thirty times larger than at the interstitial site. Satisfaction of the sum rule

$$4\pi\int dRR^2\rho_{\rm xc}^{\rm LDA}(\mathbf{r},R)=-1 \tag{16}$$

implies that if there are positive errors in $\rho_{\rm xc}^{\rm LDA}(\mathbf{r},R)$ for some R there must be negative errors for other values as can be seen clearly in Fig. 3(b). This leads to a systematic cancellation of errors[1] in the evaluation of $e_{\rm xc}^{\rm LDA}(\mathbf{r})$ in Eq. (1).

Figure 4(a) shows how the spherically averaged exchange-correlation hole changes continuously at the bond center as one turns on the correlation from $\lambda=0$ (full exchange) to $\lambda=1$ (full exchange and correlation). The hole becomes deeper with increasing Coulomb repulsion as the probability of electrons approaching one another decreases. With increasing λ the hole broadens, a trend that was observed in sine-wave jellium.[26] At each value of λ the hole satisfies the sum rule

$$4\pi\int dRR^2\rho_{\rm xc}^{\lambda}(\mathbf{r},R)=-1.$$

At $\lambda=0$ the hole is everywhere negative. With increasing λ the sum rule is satisfied by a small positive contribution that develops in $\rho_{\rm xc}^{\lambda}(\mathbf{r},R)$ at $R\approx 3$ (a.u.). In Fig. 4(b) $\rho_{\rm xc}^{\lambda}(\mathbf{r},R)$ is shown at the interstitial site. The hole becomes deeper with increasing λ with no clear trend of becoming more localized.

The WDA (Ref. 1) can be considered as a procedure that approximates $\bar{g}$ keeping the correct prefactor $n(\mathbf{r}')$ in Eq. (2) rather than $n(\mathbf{r})$ as used in the LDA,

$$\rho_{\rm xc}^{\rm LDA}(\mathbf{r},\mathbf{r}')=n(\mathbf{r})\{\bar{g}^{\rm hom}(|\mathbf{r}-\mathbf{r}'|,n(\mathbf{r}))-1\}.$$

For our comparisons we used the form of $\bar{g}$ corresponding to a homogeneous electron gas as parameterized by Perdew and Wang.[25] In this nonlocal approximation instead of using the local value of the density in the argument of the pair-correlation function at each point $\mathbf{r}$ an $\bar{n}(\mathbf{r})$ is used with a value chosen to satisfy the sum rule,

$$\int d\mathbf{r}'n(\mathbf{r}')\{\bar{g}^{\rm hom}(|\mathbf{r}-\mathbf{r}'|,\bar{n}(\mathbf{r}))-1\}=-1.$$

The quantity $e_{\rm xc}^{\rm WDA}(\mathbf{r})$ was evaluated self-consistently and the difference $e_{\rm xc}^{\rm VMC}(\mathbf{r})-e_{\rm xc}^{\rm WDA}(\mathbf{r})$ is shown in Fig. 5. Comparing with results of our previous paper,[8] which looked at deviations of the VMC from the LDA and ADA reveals that the WDA gives a better pointwise agreement of $e_{\rm xc}(\mathbf{r})$ with the VMC than the LDA with the VMC. Quantitatively the root-mean-square deviation of $e_{\rm xc}(\mathbf{r})$ from $e_{\rm xc}^{\rm VMC}(\mathbf{r})$, was 3.0% for $e_{\rm xc}(\mathbf{r})=e_{\rm xc}^{\rm WDA}(\mathbf{r})$, 4.9% for $e_{\rm xc}(\mathbf{r})=e_{\rm xc}^{\rm LDA}(\mathbf{r})$, and 2.0% for $e_{\rm xc}(\mathbf{r})=e_{\rm xc}^{\rm ADA}(\mathbf{r})$. The largest errors in the LDA occur in the bonding region where the electronic density is largest and changing rapidly, and around the pseudoatoms where it is smallest and changing rapidly. The sharp features near the extrema of the electronic density result from the local nature of $e_{\rm xc}^{\rm LDA}(\mathbf{r})$. The true nonlocal functional includes information about the charge density in the neighboring region that tends to smooth out such sharp features. For this reason the non-local ADA and WDA yield better overall agreement with our VMC result. The better agreement of the ADA with the VMC over the WDA may result from the nature of the ADA which is designed to reproduce the exact $e_{\rm xc}(\mathbf{r})$ in the limit of weak density variations while the WDA is not. The total integrated exchange-correlation energies $E_{\rm xc}$ are shown in Table II. We have combined our VMC result with a more accurate diffusion Monte Carlo calculation[27,28] to obtain a ''pure estimate,''[29] denoted DMC, of the exchange-correlation energy at $\lambda=1$, $U_{\rm xc}^{\lambda=1}$, and the kinetic energy at $\lambda=1$, $T^{\lambda=1}$. These numbers along with the kinetic energy at $\lambda=0$, $T^{\lambda=0}$, were plugged into the identity, Eq. (13), to obtain our DMC value of $E_{\rm xc}$.

The close agreement between the LDA and VMC exchange-correlation energies is due to a real-space cancellation between the bonding regions and the region around the pseudoatom and partially explains why the LDA does so well in describing silicon. Although both the ADA and the WDA give a smaller root-mean square deviation of $e_{\rm xc}(\mathbf{r})$ from $e_{\rm xc}^{\rm VMC}(\mathbf{r})$ in comparison to the LDA, they do not yield as complete a cancellation of errors as the LDA in the total $E_{\rm xc}$. The statistical error of 0.5% in the VMC evaluation of $e_{\rm xc}^{\rm VMC}(\mathbf{r})$ is an order of magnitude smaller than the deviations

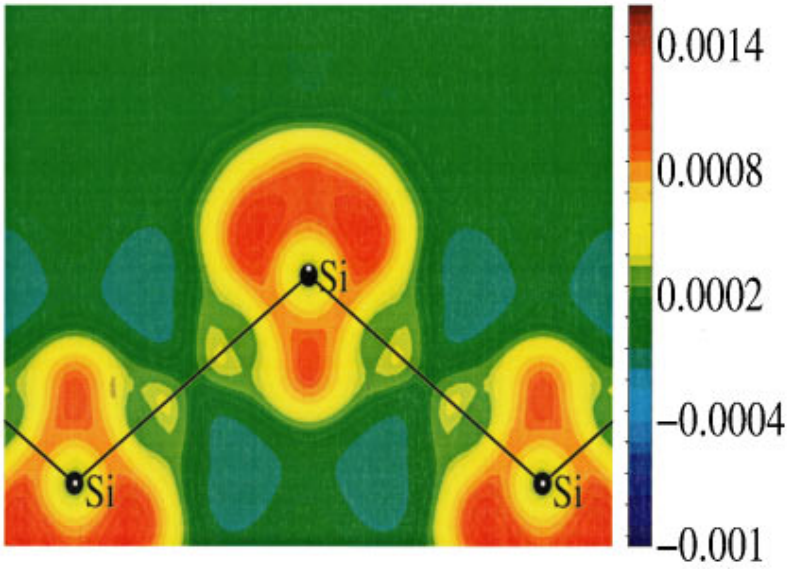

FIG. 5. (Color) Contour plot in the (110) plane passing through the atoms for $e_{xc}^{VMC}(\mathbf{r})-e_{xc}^{WDA}(\mathbf{r})$. The atoms and bonds in the (110) plane are schematically represented. The contours are in atomic units.

observed between the LDA and VMC and four times smaller than the deviations between the WDA and VMC, and ADA and VMC. (Note that the same nonlocal LDA pseudopotential was used in all schemes.)

The largest error in our VMC calculations arises from the use of approximate forms of the many-body wave functions Ψ_λ, which account for 85% of the fixed-node correlation energy at $\lambda=1$ and a larger proportion for smaller values of λ. We estimate that a DMC calculation in silicon of real-space quantities such as $e_{xc}(\mathbf{r})$ and $\rho_{xc}(\mathbf{r},\mathbf{r}')$ would require a hundredfold greater computational resources to obtain the same statistical accuracy as our VMC results. This greater cost arises from a combination of the following: (1) a smaller step length is required in DMC to reduce the time step bias, thus a greater number of steps are necessary to generate the same number of uncorrelated electron configurations, and (2) the necessity of calculating the local energy at each step. In the absence of the DMC result for $e_{xc}(\mathbf{r})$ we can only speculate how this quantity would differ from our VMC result. We would expect that an accurate physical result like the DMC would also tend to smooth out the sharp features in $e_{xc}(\mathbf{r})$ resulting from the local approximation of the LDA.

As is well known, the LDA yields values of E_x that are too large and values of E_c that are too small, resulting in a cancellation of errors. Shown in Fig. 6, $e_x^{VMC}(\mathbf{r})-e_x^{LDA}(\mathbf{r})$ reveals that LDA exchange tends to overestimate almost everywhere while $e_c^{LDA}(\mathbf{r})$ tends to underestimate almost everywhere. The exchange-correlation energy density $e_{xc}(\mathbf{r})=e_x(\mathbf{r})+e_c(\mathbf{r})$ therefore involves a cancellation between the exchange and the correlation contributions.

The cancellation between the exchange and the correlation that occurs in the LDA can be seen in more detail by studying the λ dependence of the exchange-correlation en-

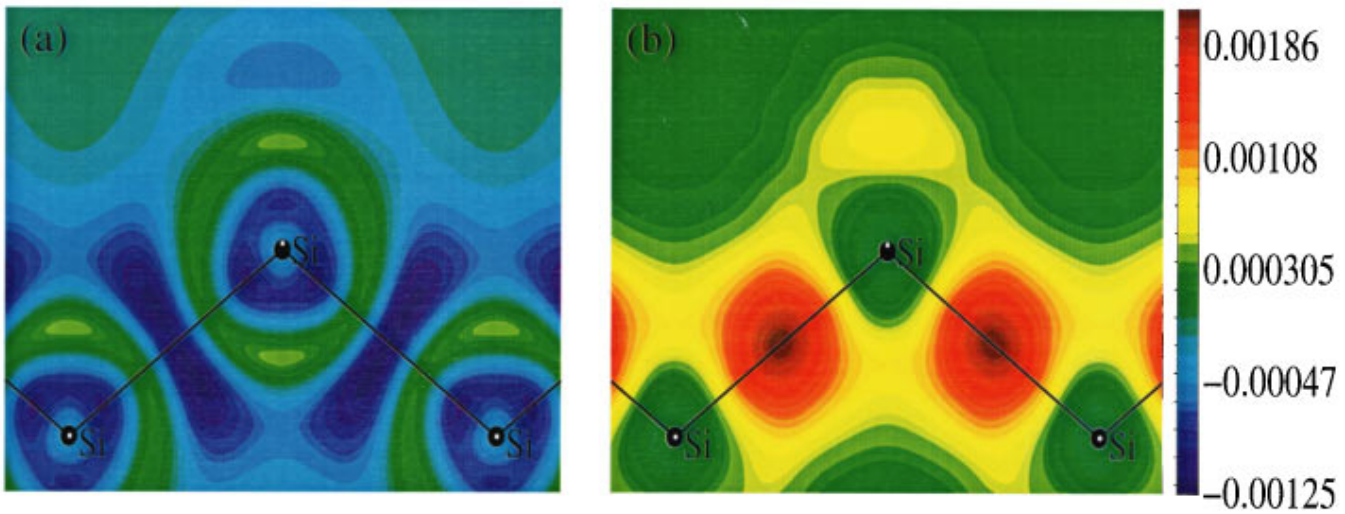

FIG. 6. (Color) Contour plots in the (110) plane passing through the atoms for (a) $e_x^{VMC}(\mathbf{r})-e_x^{LDA}(\mathbf{r})$, and (b) (a) $e_c^{VMC}(\mathbf{r})-e_c^{LDA}(\mathbf{r})$. The atoms and bonds in the (110) plane are schematically represented. The contours are in atomic units.

TABLE II. Values for the exchange energy, $E_x = U_{xc}^{\lambda=0}$, the exchange-correlation energy, $E_{xc} = \int_0^1 U_{xc}^{\lambda} d\lambda$, and $U_{xc}^{\lambda=1}$. The energies are in units of eV per atom. The statistical errors are indicated for the VMC and DMC results.

	E_x	E_{xc}	$U_{xc}^{\lambda=1}$
LDA	−27.66	−32.75	−35.64
ADA	−27.56	−32.67	−35.57
WDA	−27.37	−33.00	−36.25
GGA	−29.10	−33.03	−35.80
VMC	−29.15	−32.73 ±0.01	−34.97±0.01
DMC	−29.15	−33.23±0.08	−35.55±0.05

ergy. Shown in Fig. 7 is the Monte Carlo data compared with self-consistent calculations using different models (mod) for the exchange-correlation functional, where we used the general formula:[13]

$$U_{xc}^{\lambda,\mathrm{mod}}[n] = E_x^{\mathrm{mod}}[n] + \frac{\partial}{\partial\lambda}(\lambda^2 E_c^{\mathrm{mod}}[n_{1/\lambda}]),$$

in which $n_{1/\lambda}(x,y,z) = (1/\lambda^3)\, n(x/\lambda, y/\lambda, z/\lambda)$. All of these models with the exception of the GGA[2] over-estimate the exchange, $E_x = U_{xc}^{\lambda=0}$, while they all underestimate the correlation, $E_c = \int_0^1 d\lambda U_{xc}^{\lambda} - E_x$. The shape of these curves is important for schemes where the λ integral is approximated using a two-point integration formula[5,6] at $\lambda = 0$ and $\lambda = 1$ within some model. Detailed numerical results are shown in Table II. There is numerical evidence in atoms[30,31] that the LDA provides a more accurate description of U_{xc}^{λ} as $\lambda \to 1$. Our DMC results show closer agreement with the LDA of U_{xc}^{λ} at $\lambda = 1$ than at $\lambda = 0$ in silicon. We are currently carrying out a DMC calculation of U_{xc}^{λ} as a function of λ. We anticipate that this will introduce a negative correction to our VMC results, with a magnitude that increases monotonically with λ (no change at $\lambda = 0$ and a maximum change at $\lambda = 1$).

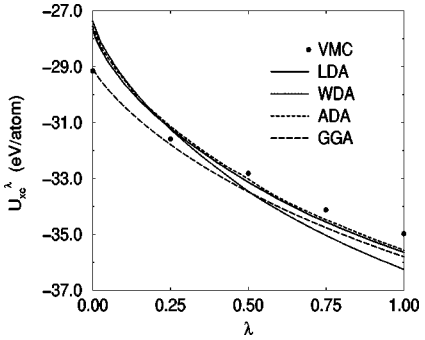

FIG. 7. Plots of U_{xc}^{λ} versus the Coulomb coupling constant λ in VMC, LDA, WDA, ADA, and GGA. The statistical error bars in VMC are smaller than the symbols.

IV. CONCLUSIONS

Coupling constant integration and VMC have been combined to calculate the principal quantities in density-functional theory that contribute to the exchange-correlation energy in silicon. The pair-correlation function was found to have a correlation contribution that was more localized and isotropic than its exchange contribution. With increasing Coulomb repulsion λ, the electron ''digs'' out a deeper exchange-correlation hole that exhibits a longer range. The success of the LDA in silicon can be viewed as a result of several errors that cancel in the evaluation of the total exchange-correlation energy,

$$E_{xc} = \int d\mathbf{r} \underbrace{\int_0^1 d\lambda \overbrace{\frac{n(\mathbf{r})}{2} \int dR\, 4\pi R \underbrace{\left[\frac{1}{4\pi}\int_\Omega d\mathbf{r}' \rho_{xc}^{\lambda}(\mathbf{r},\mathbf{r}')\right]}_{\rho_{xc}^{\lambda}(\mathbf{r},R)}}^{e_{xc}^{\lambda}(\mathbf{r})}}_{e_{xc}(\mathbf{r})}, \quad \Omega : |\mathbf{r}-\mathbf{r}'| = R \quad :$$

(1) It is sufficient to give an adequate representation of the spherical average of the exchange-correlation hole since only this averaged quantity contributes to E_{xc}. The LDA provides a much better description of the spherical average, $\rho_{xc}^{\lambda}(\mathbf{r},R)$, than $\rho_{xc}^{\lambda}(\mathbf{r},\mathbf{r}')$. (2) Performing the integral over R in the evaluation of $e_{xc}^{\lambda}(\mathbf{r})$ results in a systematic cancellation of errors, because $\rho_{xc}^{\mathrm{LDA}}(\mathbf{r},R)$ satisfies the sum rule in Eq. (16). (3) In calculating the integral over λ, we found a cancellation between the exchange contribution, $e_{xc}^{\mathrm{LDA},\lambda=0}(\mathbf{r})$, which tends to overestimate almost everywhere, with the correlation contribution [the remaining contribution to $e_{xc}^{\mathrm{LDA}}(\mathbf{r})$], which tends to underestimate almost everywhere. (4) In silicon our VMC results revealed a real-space cancellation of errors in the LDA exchange-correlation energy density $e_{xc}^{\mathrm{LDA}}(\mathbf{r})$. This cancellation partially corrects the local approximation of the LDA, which tends to exhibit sharp features, i.e., large errors, in the exchange-correlation energy density near those points in space where the charge density is rapidly varying and has an extremum. Nonlocal functionals such as the ADA and WDA, which average the density over a neighboring region, were found to smooth out these sharp features.

The computational cost of our method is much smaller than an alternative procedure for studying density-functional

theory that extracts the exchange-correlation potential by an inversion of the Kohn-Sham equations using a quantum Monte Carlo calculated electron density.[30] This alternative procedure has thus far been limited to small atoms[30,32] and model solids.[33,34] Our test calculations have revealed that the different quantities that contribute to the exchange-correlation energy are less sensitive to numerical noise and small errors in the wave function. Our method is thus immediately applicable to solids, molecules, and atoms. These and future calculations of the quantities that contribute to the exchange-correlation energy will provide a detailed and practical testing ground for new and existing functionals.

ACKNOWLEDGMENTS

We thank W. M. C. Foulkes, M. Nekovee, M. Levy, and K. Burke for helpful discussions. Financial support was provided by the Engineering and Physical Sciences Research Council (EPSRC), U.K., NSF Grant No. DMR-9157537, DOE Grant No. DE-FG02-97ER45632, and NATO Collaborative Research Grant No. CRG.951105. Our calculations were performed on the Cray-T3D at EPCC, the Cray-T3D at PSC under Grant No. DMR-960004P, the Hitachi SR2001 located at Hitachi Europe's Maidenhead headquarters, and the Hitachi SR2201 located at the University of Cambridge High Performance Computing Facility.

APPENDIX

At each λ a sum rule satisfied by the pair-correlation function has the form

$$\sum_{\beta} \int d\mathbf{r}' n_{\beta}^{\lambda}(\mathbf{r}')\{g_{\alpha\beta}^{\lambda}(\mathbf{r},\mathbf{r}')-1\}=-1, \qquad \text{(A1)}$$

where $n_{\beta}^{\lambda}(\mathbf{r}')$ and $g_{\alpha\beta}^{\lambda}(\mathbf{r},\mathbf{r}')$ are the spin-dependent components of the density and the pair-correlation function respectively, sampled from the same wave function. In this appendix the λ dependence of the density is made explicit. The small differences (less than 0.58%) between n_{λ} and $n_{\lambda=1}$ do not show up in plots of the exchange-correlation hole but can have an effect on $e_{\mathrm{xc}}(\mathbf{r})$ if not treated properly. Here we define the quantity:

$$\tilde{n}_{\alpha}^{\lambda}(\mathbf{r})=n_{\alpha}^{\lambda}(\mathbf{r})\left(\frac{\sum_{\beta}\int d\mathbf{r}' n_{\beta}^{\lambda}(\mathbf{r}')g_{\alpha\beta}^{\lambda}(\mathbf{r},\mathbf{r}')}{N-1}\right),$$

using the statistically sampled expansion, Eq. (11), for $g_{\alpha\beta}^{\lambda}(\mathbf{r},\mathbf{r}')$. In general $\tilde{n}_{\alpha}(\mathbf{r})\neq n_{\alpha}(\mathbf{r})$ since the statistical noise, as described in Sec. II D, can lead to violations of the sum rule, Eq. (A1), at each $\mathbf{r}$. Next we define a new pair-correlation function:

$$\tilde{g}_{\alpha\beta}^{\lambda}(\mathbf{r},\mathbf{r}')=\frac{n_{\alpha}(\mathbf{r})n_{\beta}(\mathbf{r}')}{\tilde{n}_{\alpha}(\mathbf{r})\tilde{n}_{\beta}(\mathbf{r}')}g_{\alpha\beta}^{\lambda}(\mathbf{r},\mathbf{r}')$$

and a corresponding exchange-correlation hole,

$$\tilde{\rho}_{\mathrm{xc},\alpha\beta}^{\lambda}(\mathbf{r},\mathbf{r}')=\tilde{n}_{\beta}^{\lambda}(\mathbf{r}')\{\tilde{g}_{\alpha\beta}^{\lambda}(\mathbf{r},\mathbf{r}')-1\}.$$

Utilizing the orthonormality of the basis functions $\phi_{tr,m}^{\mathbf{k}p}(\mathbf{r})$, a new set of coefficients can be obtained for an expansion in the form of Eq. (11) for $\tilde{g}_{\alpha\beta}^{\lambda}(\mathbf{r},\mathbf{r}')$. By construction the sum rule

$$\sum_{\beta}\int d\mathbf{r}'\tilde{n}_{\beta}^{\lambda}(\mathbf{r}')\{\tilde{g}_{\alpha\beta}^{\lambda}(\mathbf{r},\mathbf{r}')-1\}=-1$$

is satisfied. The deviations of $\tilde{n}^{\lambda}(\mathbf{r})$ from $n^{\lambda=1}(\mathbf{r})$ are the same size as the deviations of $n^{\lambda}(\mathbf{r})$ from $n^{\lambda=1}(\mathbf{r})$. The small differences observed between $\tilde{g}_{\alpha\beta}^{\lambda}(\mathbf{r},\mathbf{r}')$ and $g_{\alpha\beta}^{\lambda}(\mathbf{r},\mathbf{r}')$ are only discernable when $\mathbf{r}$ is far from $\mathbf{r}'$ where $g_{\alpha\beta}^{\lambda}(\mathbf{r},\mathbf{r}')\approx 1$. However, the quantity $e_{\mathrm{xc}}(\mathbf{r})$ is sensitive to whether one uses $\rho_{\mathrm{xc}}^{\lambda}$ or $\tilde{\rho}_{\mathrm{xc}}^{\lambda}$ in Eq. (15), with the choice of $\tilde{\rho}_{\mathrm{xc}}^{\lambda}$ resulting in smaller statistical errors.

*Present address: Cavendish Laboratory, Madingley Road, Cambridge CB3 0HE, U.K.

†Present address: National Renewable Energy Laboratory, Golden, Colorado 80401.

[1] O. Gunnarsson, M. Jonson, and B. I. Lundqvist, Phys. Rev. B **20**, 3136 (1979).

[2] J. P. Perdew in *Electronic Structure of Solids '91*, edited by P. Ziesche and H. Eschrig (Akademie Verlag, Berlin, 1991); J. P. Perdew and Y. Wang (unpublished).

[3] A. Görling, Phys. Rev. B **53**, 7024 (1996).

[4] T. Grabo and E. K. U. Gross, Chem. Phys. Lett. **240**, 141 (1995).

[5] A. D. Becke, J. Chem. Phys. **98**, 1372 (1993).

[6] A. D. Becke, J. Chem. Phys. **88**, 1053 (1988).

[7] A. Görling and M. Levy, J. Chem. Phys. **106**, 2675 (1997).

[8] R. Q. Hood, M. Y. Chou, A. J. Williamson, G. Rajagopal, R. J. Needs, and W. M. C. Foulkes, Phys. Rev. Lett. **78**, 3350 (1997).

[9] For a derivation see, for example, R. M. Dreizler and E. K. Gross, *Density Functional Theory, An Approach to the Quantum Many-Body Problem* (Springer-Verlag, Berlin, 1990), pp. 183–185.

[10] We use Hartree atomic units ($\hbar=e=m=4\pi\epsilon_0=1$) for all equations.

[11] A. J. Williamson, G. Rajagopal, R. J. Needs, L. M. Fraser, W. M. C. Foulkes, Y. Wang, M. Y. Chou, Phys. Rev. B **55**, R4851 (1997); L. M. Fraser, W. M. C. Foulkes, G. Rajagopal, R. J. Needs, S. D. Kenny, and A. J. Williamson, *ibid.* **53**, 1814 (1996).

[12] Z. W. Lu, A. Zunger, and M. Deutsch, Phys. Rev. B **47**, 9385 (1993); J. M. Zuo, P. Blaha, and K. Schwarz, J. Phys.: Condens. Matter **9**, 7541 (1997).

[13] A. Görling and M. Levy, Phys. Rev. B **47**, 13 105 (1993).

[14] In principle, one should reduce the deviations in the density relative to $n_{\lambda=1}(\mathbf{r})$. However, we were unable to distinguish the small differences between $n_{\lambda=1}$ and n_{LDA} from the residual statistical noise.

[15] A. J. Williamson, S. D. Kenny, G. Rajagopal, A. J. James, R. J. Needs, L. M. Fraser, W. M. C. Foulkes, and P. Maccallum, Phys. Rev. B **53**, 9640 (1996).

[16] C. J. Umrigar, K. G. Wilson, and J. W. Wilkins, Phys. Rev. Lett. **60**, 1719 (1988).

[17] S. Fahy, X. W. Wang, and S. G. Louie, Phys. Rev. B **42**, 3503 (1990).
[18] S. Fahy, X. W. Wang, and S. G. Louie, Phys. Rev. Lett. **65**, 1478 (1990).
[19] Here we are following the notation as used in J. F. Cornwell, *Group Theory in Physics*, edited by N. H. March (Academic Press, London, 1984), Vol. 1, pp. 222–245.
[20] J. F. Cornwell, *Group Theory in Physics*, edited by N. H. March (Academic Press, London, 1984), Vol. 1, p. 81.
[21] J. F. Cornwell, *Group Theory and Electronic Energy Bands in Solids* (North-Holland, Amsterdam, 1969), pp. 137–143.
[22] M. Levy and J. P. Perdew, Phys. Rev. A **32**, 2010 (1985).
[23] A. K. Rajagopal, J. C. Kimball, and M. Banerjee, Phys. Rev. B **18**, 2339 (1978).
[24] For a discussion of this and other definitions of the exchange and correlation functionals of density-functional theory, we refer the reader to V. Sahni and M. Levy, Phys. Rev. B **33**, 3869 (1986).
[25] J. P. Perdew and Y. Wang, Phys. Rev. B **46**, 12947 (1992).
[26] M. Nekovee, W. M. C. Foulkes, A. J. Williamson, G. Rajagopal, and R. J. Needs, Adv. Quantum Chem. (to be published), thematic volume on DFT, edited by J. M. Seminario.
[27] D. Ceperley, G. V. Chester, and M. H. Kalos, Phys. Rev. B **16**, 3081 (1971).
[28] B. L. Hammond, W. A. Lester, Jr., and P. J. Reynolds, *Monte Carlo Methods in ab initio Quantum Chemistry* (World Scientific, Singapore, 1994).
[29] D. M. Ceperley and M. H. Kalos, in *Monte Carlo Methods in Statistical Physics*, edited by K. Binder (Springer-Verlag, New York, 1979), pp. 183–185.
[30] C. J. Umrigar and X. Gonze, in *High Performance Computing and its Applications to the Physical Science*, Proceedings of the Mardi Gras '93 Conference, edited by D. A. Browne *et al.* (World Scientific, Singapore, 1993).
[31] C. Filippi, X. Gonze, and C. J. Umrigar, in *Recent Developments and Applications of Modern Density Functional Theory*, edited by J. Seminario (Elsevier, Amsterdam, 1996).
[32] C. Filippi, C. J. Umrigar, and X. Gonze, Phys. Rev. A **54**, 4810 (1996).
[33] W. Knorr and R. W. Godby, Phys. Rev. Lett. **68**, 639 (1992).
[34] G. E. Engel, Y. Kwon, and R. M. Martin, Phys. Rev. B **51**, 13 538 (1995).